CrossMark

AFSTi
Empowering food professionals

ORIGINAL ARTICLE

Characterization of swiftlet edible bird nest, a mucin glycoprotein, and its adulterants by Raman microspectroscopy

Eric K. S. Shim[1] · Gleen F. Chandra[1] · S. Pedireddy[1] · Soo-Y. Lee[1]

Abstract Edible bird's nest (EBN) is made from the glutinous salivary secretion of highly concentrated mucin glycoprotein by swiftlets (genus *Aerodramus* or *Collocalia*) native to the Indo-Pacific region. The unique Raman spectrum of EBN has vibrational lines that can be assigned to peptides and saccharides in the glycoprotein, and it can be used to screen for adulteration. The common edible adulterants classified into two types. Type I adulterants, such as fish bladder, pork skin, karaya gum, coralline seaweed, agar strips, and tremella fungus, were solids which adhered *externally* on the surface of the EBN cement. They can usually be detected with a microscope based on differences in the surface structure. Type II adulterants were water soluble substances such as saccharides (e.g., glucose, sucrose), polypeptides (e.g., hydrolyzed collagen) and salts (e.g. monosodium glutamate) which can be readily soaked up by the EBN hydrogel when moist and adsorbed *internally* in the EBN cement matrix forming a composite upon drying, making them difficult to detect visually. The present study showed that Raman microspectroscopy offers a rapid, non-invasive, and label free technique to detect both Type I and II adulterants in EBN.

Keywords Edible bird's nest · Raman microspectroscopy · Mucin glycoprotein · Adulterants · Characterisation

✉ Soo-Y. Lee
sooying@ntu.edu

1   Division of Chemistry and Biological Chemistry, School of Physical and Mathematical Sciences, Nanyang Technological University, 21 Nanyang Link, Singapore 637371, Singapore

Introduction

Raw white edible bird's nest (EBN), also known as cubilose or nest cement, is a relatively strong, hardened, composite material made mainly of dried strands of amorphous mucin glycoprotein, secreted by male swiftlets of genus *Aerodramus* or *Collocalia* during the nesting and breeding season from a pair of sublingual glands under the tongue. The strands are bound together with feathers, and occasionally impregnated with tiny sand grains regurgitated from the birds gizzard, making a strong composite material to bear the weight of the nestlings. These swiftlets are native to the Indo-Pacific region and commonly found in South-East Asian countries, predominantly in Indonesia, Malaysia, Thailand and Vietnam. The raw EBN, carefully cleaned of feathers, sand grains, etc., by soaking and picking of impurities with tweezers, besides being a Chinese food delicacy, has been a part of traditional Chinese medicine for more than 1000 years, and is reputed to have nutritional and medicinal properties (Guo et al. 2006; Haghani et al. 2016; Vimala et al. 2012).

Analysis of EBN using modern chemical methods can be traced back to 1921 where it was shown that EBN is a mucin glycoprotein with properties of both carbohydrate and protein (Wang 1921). Structurally, a glycoprotein is a dendritic polymer, like a bottle brush, with a polypeptide backbone and hundreds of polysaccharide chains attached to it by O- or N-glyosidic linkages, and has molecular weight of 40–130 kDa (Wieruszeski et al. 1987). By proximate analysis on EBN (Marcone 2005), it was found that the protein portion constitutes $\sim 62\%$ by weight and is made up of 17 types of amino acids, with serine, valine, isoleucine, tyrosine, aspartic acid and asparagines as the major components, but with an absence of proline and two essential amino acids—tryptophan and cysteine. The

carbohydrate portion makes up ∼28 % by weight, and the major saccharides are sialic acid (*N*-acetylneuraminic acid), galactose, *N*-acetylgalactosamine, *N*-acetylglucosamine, fucose and mannose. The rest are moisture (∼8 %), ash/minerals (∼2 %), and fat (<1 %).

A kilogram of the cleaned white EBN retails for more than USD 1500 per kg today as the supply is limited due to the labour intensive manual cleaning process, increasing labour cost, and high demand for EBN especially in China with growing affluence among the population. Given a global output of about a million kg per year, this translates to a trade worth USD 1.5 billion per year. The high price of EBN is an inducement for EBN processors to adulterate it to increase profits. Consumers and retailers often rely on sight and smell to try to pick out the genuine EBN. It is often difficult to detect adulterated EBN by such simple (macroscopic) physical means, especially when the adulteration level is no more than 10 % by weight. An official or standard method has yet to be found for the authentication and quality surveillance of EBN.

Various physical, analytical and chemical techniques have been designed to check for the presence of adulterants in EBN. The authentication techniques so far can generally be classified under: microscopy (Marcone 2005; Yang et al. 2014), chromatography (Chua et al. 2015; Hun et al. 2016), spectroscopy (Ma and Liu 2012; Marcone 2005), enzymatic and genomic methods (Yang et al. 2014; Zhang et al. 2013), and qualitative analysis (Marcone 2005). However, most of the techniques are invasive, require tedious sample preparation, slow and generally not easy to use.

The edible adulterants in EBN into two types: (a) *Type I adulterants* are solid substances with similar appearance and can be adhered *externally* to the EBN cement. (b) *Type II adulterants* are incorporated *internally* into the EBN cement matrix, and not yet discussed in the literature. They are water soluble substances that can be absorbed by the moist EBN hydrogel and are embedded in the EBN cement to form a composite upon drying. The hydrogel character of EBN arises from the presence of hydrophilic polysaccharides in the glycoprotein polymer, and the EBN cement can soak up about five times its weight of moisture at room temperature. Based on the EBN mucin glycoprotein structure, adulterants can be carbohydrates, proteins, other glycoproteins, or salts. Typical Type I adulterants are solid polysaccharides (karaya gum, *tremella fungus*, coralline seaweed, agar strips) and polypeptides (fish bladder, pork skin), while the common Type II adulterants are water soluble saccharides (e.g. glucose, sucrose), polypeptides (e.g. hydrolyzed marine collagen), and salts (e.g. monosodium glutamate).

Edible adulterants are incorporated into the cleaned EBN to increase its weight, and Type I adulterants may be introduced by up to 10 % in weight to evade detection with the naked eye. Type I adulterants which are external to the EBN cement, however, can be detected with a microscope due to differences in their surface structure. Type II adulterants which are embedded in the EBN cement are more covert and difficult to detect visually. More sophisticated techniques and tools are required to identify and detect Type II adulterants.

Spectroscopic methods can provide a simple, non-invasive and fast way to detect both Type I and II adulterants. Fourier transform infrared (FTIR) spectroscopy, an absorption technique, has been used for detecting Type I adulterants which can be picked out from the EBN by examining the bands of the adulterants in the fingerprint region. If the adulterants are embedded in the EBN cement in small amounts, as in the case of Type II adulterants, FTIR might not be sensitive enough to detect the adulterants.

Raman spectroscopy is a scattering technique, complementary to absorption FTIR, often able to give a richer vibrational spectrum with sharper lines due to differences in spectral selection rules. It is non-invasive, applicable to opaque samples, is not affected by moisture in the sample, but has yet to be employed as an authentication method of EBN. The frequencies of the Raman lines correspond to vibrational modes in a molecule, and each molecule has a distinct set of vibrational modes. The intensity of a Raman line is proportional to the concentration of the molecule present. Hence the vibrational fingerprint of both frequency and intensity in Raman spectroscopy is routinely used in analysis to determine the kind of molecule and its concentration. Raman microspectroscopy, with spatial resolution of about 1 μm, also has an advantage over FTIR in being able to focus on tiny spots over various regions of the sample, and therefore it is a good tool to identify both Type I and II adulterants that may either be lumpy or uniformly distributed across the EBN cement. Raman spectroscopy has been used successfully in food analysis and in the study of various agricultural products (Martin et al. 2015; Pereira et al. 2003; Yang and Ying 2011). The aim of this work was to investigate the potential of Raman microspectroscopy as a rapid, non-invasive, and label free technique for studying EBN and detecting adulterants in EBN.

Materials and methods

Edible bird's nest (EBN) samples

Raw, white EBN samples produced by *Aerodramus fuciphagus* were obtained from bird houses in widely separated geographical locations in South-East Asia—Kuantan (West Malaysia), Kuching (East Malaysia), and Jakarta (Indonesia).

Raman microspectroscopy

Raman spectra were collected with the Ramantouch microspectrometer (Nanophoton Inc, Osaka, Japan) with a CCD detector, using a linearly polarized 785 nm laser as an excitation laser, with a spectral grating of 600 gr/mm and an excitation power of 140 mW on the sample. A clear piece of EBN sample was placed on a silicon substrate glass slide and the Raman spectrum was collected in the range 724–1800 cm^{-1}.

The spectra were calibrated with the 520 cm^{-1} silicon peak. The Origin Pro 8.0 software was used to make the baseline correction. The excitation laser light was focused into a single spot on the sample through a cylindrical lens and an air objective lens (LU Plan Fluor 20×, NA 0.45). The back-scattered Raman signal from the spot-illuminated site was collected with the same objective lens. The exposure time for each spot was 60 s.

Adulterant samples

Tremella fungus, coralline seaweed, Japanese agar strips, fish bladder, pork skin, glucose, sucrose, and monosodium glutamate were purchased from grocery stores. Karaya gum, and hydrolyzed marine collagen were purchased from suppliers of food chemicals and ingredients. Ultrapure water used in experiments was generated with the Merck Millipore ultrapure water system.

Uptake of Type II adulterants by EBN

About 1 g of EBN was carefully weighed and soaked overnight in 50 mL of 10 % w/w aqueous solutions of glucose, sucrose, hydrolyzed marine collagen, and monosodium glutamate. The EBN samples were sieved, rinsed with ultrapure water and air-dried with fan to constant weight (about 3 days) at a room temperature of 24 °C and under relative humidity of about 50 %, simulating conditions used by EBN processors. The samples were weighed to estimate the amount of adulterant that was absorbed by and embedded in the EBN cement. Five samples were prepared for each adulterant. Raman spectra were taken on the dried samples.

Results and discussion

Raman spectra of EBN

The Raman spectra of the EBN samples from geographically different places—Kuantan (West Malaysia), Kuching (East Malaysia), and Jakarta (Indonesia)—are shown in Fig. 1. They show identical vibrational bands in the fingerprint region, suggesting that they are generally made of the same material by the same species of swiftlets.

The Raman lines, shown in Fig. 1, were assigned using data for other glycoproteins (Ashton et al. 2013), soy protein isolate (Herrero et al. 2009), tyrosine (Hernández et al. 2016), collagens (Nguyen et al. 2012), and N-acetylneuraminic acid, a sialic acid (Vinogradova et al. 2014). The Raman spectrum of EBN clearly shows that it is a glycoprotein with vibrational lines of both peptides and sacharides. Table 1 gives a summary of the vibrational lines and assignments.

Type I adulterants

Although Type I adulterants, being solids with different surface structure from EBN, can be picked out using a microscope, Raman microspectroscopy offers a definitive way to identify Type I adulterants as each has a unique Raman spectrum different from that of genuine EBN. The Raman spectra of the common Type I adulterants—fish bladder and pork skin which are largely collagens (protein); karaya gum, coralline seaweed and Japanese agar which are polysaccharides; and tremella fungus which is largely a polysaccharide—in comparison to an unadulterated EBN sample are shown in Fig. 2. The fish bladder and pork skin would have the polypeptide amide lines, but generally lack the polysaccharide lines, and so they differ significantly from EBN in the 1300–1400, 1050–1150 and 800–980 cm^{-1} regions. There was also a relatively higher concentration of phenylalanine in EBN (intense 1003 cm^{-1} line) compared to the collagens. The karaya gum, coralline seaweed and Japanese agar, being polysaccharides, lack the strong Amide I band at 1671 cm^{-1}, the strong C–H deformation of polypeptide band at 1446 cm^{-1}, and the strong phenylalanine ring vibration at 1003 cm^{-1} of EBN. The composition of tremella fungus is largely carbohydrate (78.3 %) with a small amount of protein (6.6 %) and crude fibre, and so the Raman spectrum would be more like that of the polysaccharides. The characteristic Raman bands of Type I adulterants are summarized in Table 2.

Type II adulterants

Four common kinds of Type II adulterants are glucose, sucrose, (hydrolyzed marine) collagen, and monosodium glutamate (MSG). Fructose can also be a Type II adulterant, but it is not used because it can more readily undergo a Maillard reaction with the amino acids present in EBN, which may lead to undesirable coloration in the presence of heat. Type II adulterants in solution can be absorbed by the EBN hydrogel. EBN samples were soaked in the 10 % w/w aqueous solutions of the adulterants overnight. It is useful to note that bottled EBN, a popular Asian tonic drink,

Fig. 1 Unique Raman spectra of EBN samples collected from different geographical locations. *A* Kuantan, West Malaysia (*black line*), *B* Kuching, East Malaysia (*red line*), *C* Jakarta, Indonesia (*orange line*). The band assignments attributed to peptides are shown in *black*, and those that are attributed to saccharides are shown in *red* (color figure online)
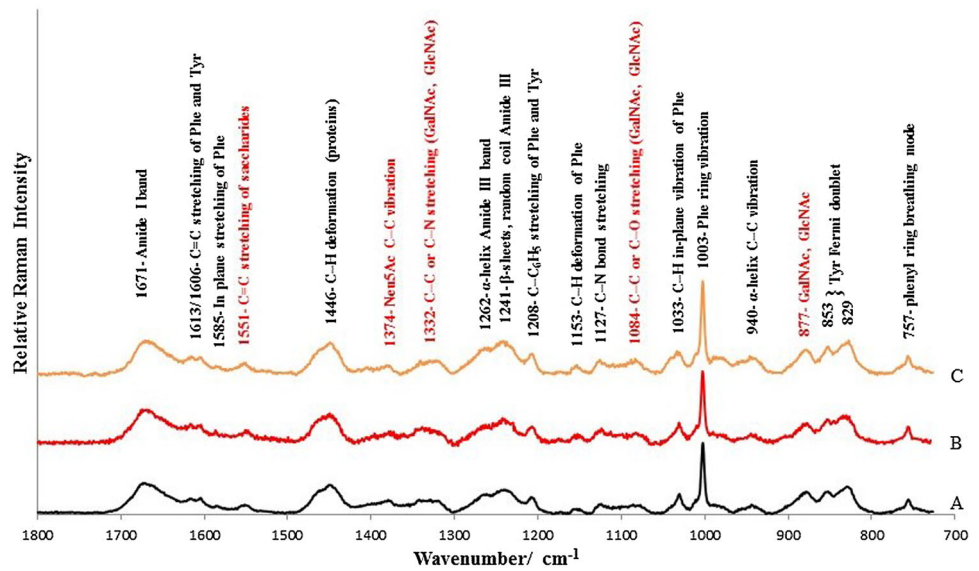

Table 1 Assignment of vibrational lines in the EBN Raman spectrum

Raman shift (cm^{-1})	Contributor	Assignments
1671 (s)	Peptide	Amide I band
1613 (m)	Peptide	C=C stretching of Phe and Tyr
1606 (m)	Peptide	C=C stretching of Phe and Tyr
1585 (w)	Peptide	In plane stretching of Phe
1551 (w)	Saccharide	C=C stretching of saccharides
1446 (s)	Peptide	C–H deformation (proteins)
1374 (w)	Saccharide	Neu5Ac C–C vibration
1332 (w)	Saccharide	C–C or C–N bond stretching (GalNAc, GlcNA)
1262 (m)	Peptide	α-Helix amide III band
1241 (s)	Peptide	β-Sheets, random coil Amide III
1208 (m)	Peptide	C–C$_6$H$_5$ stretching of Phe and Tyr
1153 (w)	Peptide	C–H deformation of Phe
1127 (w)	Peptide	C–N bond stretching (proteins)
1084 (m)	Saccharide	C–C or C–O bond stretching (GalNAc, GlcNAc)
1033 (s)	Peptide	C–H in-plane vibration of Phe
1003 (vs)	Peptide	Phe ring vibration
940 (w)	Peptide	α-Helix C–C vibration
877 (s)	Saccharide	GalNAc, GlcNAc
853 (s)	Peptide	Tyr Fermi doublet
829 (s)	Peptide	Tyr Fermi doublet
757 (m)	Peptide	Phenyl ring breathing mode

would contain added sweeteners like sucrose and glucose, supplements like collagen, and taste enhancers like MSG. The EBN, acting as a hydrogel, absorbs about 5 times its weight of solution and expands. The moist EBN was fan dried to constant weight as described above, and the adulterant was left behind, adsorbed together with some

water in the glycoprotein chains of the EBN cement to form an amorphous composite material. The average weight increases for five runs of each adulterant were as follows: glucose (34 ± 10 %), sucrose (66 ± 15 %), collagen (42 ± 10 %), and MSG (26 ± 8 %). Experiments were also carried out where the EBN was soaked in 5 %

w/w aqueous solutions of the adulterants overnight, and the average weight increases were about half that for the 10 % w/w aqueous solutions. The weight increase is largely due to adsorbed adulterant, as can be shown by thermo-gravimetric analysis which will be reported in a future study. The adsorption of the adulterants in EBN by weight percentage shows the following order: sucrose > glucose ∼ collagen > MSG. Or, generally, saccharides > peptides > salts, which can be explained by the structure of the EBN glycoprotein which has a polypeptide backbone with numerous polysaccharide chains attached to it and saccharides are more easily adsorbed on the exposed polysaccharide chains.
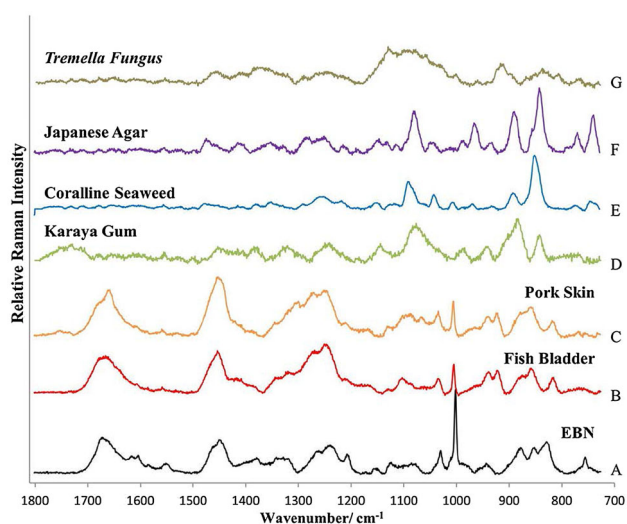

Fig. 2 Raman spectra of common Type I adulterants compared to EBN. *A* EBN from Kuantan (*black line*), *B* Fish bladder (*red line*), *C* Pork skin (*orange line*), *D* Karaya gum (*green line*), *E* Coralline seaweed (*blue line*), *F* Japanese agar (*purple line*), *G* Tremella fungus (*brown line*). Sample A is a glycoprotein; Samples B and C are collagens, i.e. proteins; while Samples D–G are largely polysaccharides (color figure online)

There was generally no observable change in physical appearance of the EBN strands after the absorption of the Type II adulterants, except for salts which may leave some shiny crystals on the surface of the EBN strands, as seen through the microscope of the Raman instrument. The Raman spectra of the adulterated EBN (blue line), the unadulterated EBN (black line), the difference spectrum between the adulterated and unadulterated EBN (red line), and the pure adulterant (green line), are shown in Fig. 3. Clearly, the difference spectra (red line) show the main bands of the pure adulterants. The boxes in each figure show the regions where the Raman spectrum of the adulterated EBN differ from the unadulterated EBN, with new lineshapes, intensities, or new lines which are attributed to the additional Raman scattering by the adsorbed adulterant, and they are summarized in Table 3.

Generally, new lines appear for the adulterated EBN in regions where the Raman bands for the pure adulterant are relatively strong. They may not occur exactly at the same frequencies as those in the pure adulterant and the bands may also be broadened, indicating that physical adsorption and caging of the adulterant molecules has occurred forming a composite material with the amorphous EBN. The strong Raman intensity of the band at 1130 cm^{-1} for glucose and at 850 cm^{-1} for sucrose (Ilaslan et al. 2015; Mathlouthi and Vinh Luu 1980; Söderholm et al. 1999), as seen in Fig. 3, can be used for quantification of glucose and sucrose adsorbed in EBN, with the construction of a calibration curve as in a Beer-Lambert plot for absorbance versus concentration. Interestingly, the Raman spectrum of marine collagen, a common supplement taken for skin health, has many spectral similarities to EBN due to similar amino acid constituents, which would make it a choice adulterant. The Raman spectrum of EBN + MSG also has many similarities to unadulterated EBN because there are no strong protein or saccharide bands in MSG. However, there are still frequency regions where the spectra of the EBN + adulterant differ sufficiently in lineshape and

Table 2 Characteristic Raman bands of common Type I adulterants

Type I adulterants	Characteristic Raman band (cm^{-1})
Fish bladder	1668 (s), 1654 (s), 1448 (s), 1411 (m), 1306 (sh), 1263 (sh), 1243 (s), 1099 (m), 1028 (m), 1003 (s), 933 (m), 917 (s), 874 (m), 853 (m)
Pork skin	1669 (s), 1654 (s), 1448 (s), 1411 (m), 1263 (sh), 1240 (s), 1094 (m), 1028 (m), 1001 (s), 930 (m), 917 (m), 877 (m), 851 (m), 810 (m)
Karaya gum	1729 (m), 1446 (m), 1377 (m), 1318 (m), 1240 (m), 1147 (m), 1070 (s), 983 (m), 989 (m), 882 (s), 840 (s)
Coralline seaweed	1249 (m), 1090 (s), 1040 (m), 889 (m), 849 (vs)
Japanese agar–agar	1471 (m), 1079 (s), 963 (m), 890 (s), 837 (s), 770 (m), 738 (m)
Tremella fungus	1452 (m), 1374 (m), 1126 (s), 1087 (s), 1074 (s), 1056 (m), 910 (m)

intensity from that of unadulterated EBN for collagen and MSG, as shown by the boxes in Fig. 3.

A principal component analysis (PCA) of all the Raman spectra comprising the EBN + Adulterant Raman spectra,
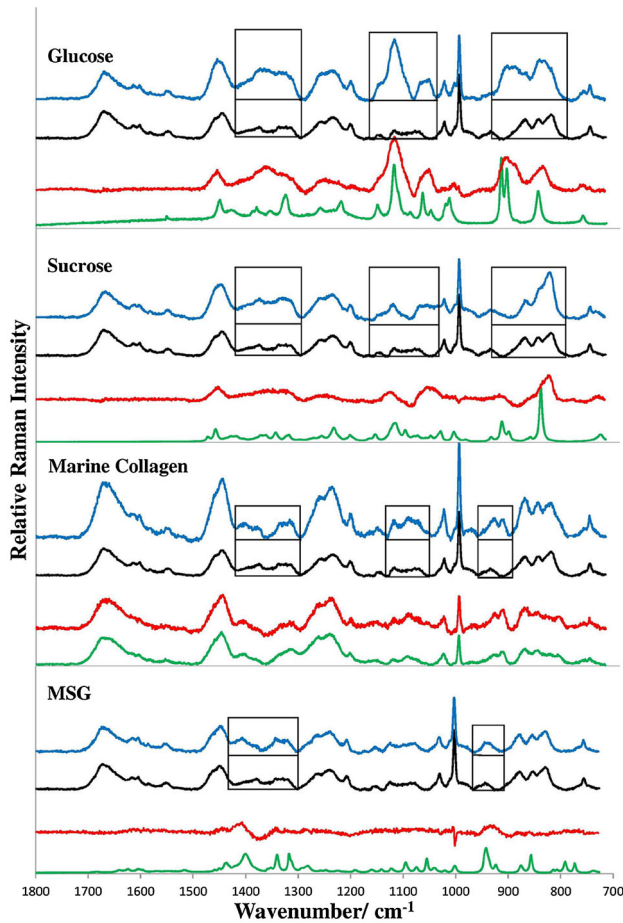

Fig. 3 Comparison of Raman spectra of EBN adulterated with Type II adulterants (*blue line*) unadulterated EBN (*black line*), the difference spectra (*red line*) and the pure adulterant (*green line*). The adulterants, from *top* to *bottom*, are glucose, sucrose, hydrolyzed marine collagen and monosodium glutamate (MSG). The *rectangular boxes* show the spectral regions where the adulterated EBN differ from the unadulterated EBN in *lineshape* and intensity, and they are due to the additional Raman scattering of the adsorbed adulterant (color figure online)

for samples soaked in 5 and 10 % w/w aqueous solutions of the adulterants, Raman spectrum of hydrolyzed marine collagen, and the unadulterated EBN Raman spectra from four different geographical regions, using the intensities of the Raman lines with frequencies listed in Tables 1 and 3, was carried out. From the PCA score plot, we can distinguish two clusters. One cluster for EBN adulterated with glucose and sucrose is due to the characteristic strong Raman bands at 1130 cm^{-1} (glucose) and 830 cm^{-1} (sucrose) arising from the CH out-of-plane deformation with the peptide bands of EBN relatively unchanged in frequency and intensity. A second cluster is for the rest of the samples. The Raman spectrum for marine collagen is very close to that of EBN in band frequencies with minor differences in relative intensities, and most of the strong bands are contributed by peptides which are the major components in EBN and marine collagen. The Raman bands for MSG are relatively weak and therefore the dominant Raman bands in EBN + MSG arise from EBN. These commonalities explains the second cluster.

Conclusion

The common adulterants of EBN have been categorized into Type I and II. Within each type, the adulterants may be largely saccharides or peptides. Type I adulterants which were external to the EBN cement can be detected with a microscope whereas water soluble Type II adulterants were physically adsorbed into the EBN cement matrix to form a composite and were not visible microscopically. Raman microspectroscopy was observed to be a simple, fast, effective, and non-destructive way to analyze both Type I and Type II adulterants in EBN. It was also observed that saccharides (glucose, sucrose), peptides (hydrolyzed marine collagen), and salt (MSG) were physically adsorbed and embedded in the glycoprotein chains of the EBN. This functionality of EBN as a hydrogel can be further explored in future as nutritious substrate for drug delivery.

Table 3 Frequency ranges where the Raman spectra of adulterated EBN differ from the unadulterated EBN, and new Raman lines for the adulterated EBN

Type (II) adulterants	Frequency ranges (cm^{-1}) where Raman spectra are significantly different from unadulterated EBN	New lines (cm^{-1})
Glucose	1425–1300, 1160–1050, 925–780	1115 (vs), 1060 (m), 900 (s), 825 (s)
Sucrose	1425–1300, 1165–1050, 925–780	1135 (m), 830 (s)
Hydrolyzed marine collagen	1425–1300, 1130–1050, 960–890	1406 (w), 1323 (m), 1100 (m), 920 (m)
Monosodium glutamate (MSG)	1430–1300, 970–910	1410 (m), 1341 (m), 940 (m)

References

Ashton L, Pudney PDA, Blanch EW, Yakubov GE (2013) Understanding glycoprotein behaviours using Raman and Raman optical activity spectroscopies: characterising the entanglement induced conformational changes in oligosaccharide chains of mucin. Adv Colloid Interface Sci 199–200:66–77. doi:10.1016/j.cis.2013.06.005

Chua YG, Chan SH, Bloodworth BC, Li SFY, Leong LP (2015) Identification of Edible Bird's Nest with Amino Acid and Monosaccharide Analysis. J Agric Food Chem 63:279–289. doi:10.1021/jf503157n

Guo C-T et al (2006) Edible bird's nest extract inhibits influenza virus infection. Antivir Res 70:140–146. doi:10.1016/j.antiviral.2006.02.005

Haghani A, Mehrbod P, Safi N, Aminuddin NA, Bahadoran A, Omar AR, Ideris A (2016) In vitro and in vivo mechanism of immunomodulatory and antiviral activity of Edible Bird's Nest (EBN) against influenza A virus (IAV) infection. J Ethnopharmacol 185:327–340. doi:10.1016/j.jep.2016.03.020

Hernández B, Coïc Y-M, Pflüger F, Kruglik SG, Ghomi M (2016) All characteristic Raman markers of tyrosine and tyrosinate originate from phenol ring fundamental vibrations. J Raman Spectrosc 47:210–220. doi:10.1002/jrs.4776

Herrero AM, Jiménez-Colmenero F, Carmona P (2009) Elucidation of structural changes in soy protein isolate upon heating by Raman spectroscopy. Int J Food Sci Technol 44:711–717. doi:10.1111/j.1365-2621.2008.01880.x

Hun LT et al (2016) Gel electrophoretic and liquid chromatographic methods for the identification and authentication of cave and house edible bird's nests from common adulterants. Anal Methods 8:526–536. doi:10.1039/C5AY02170G

Ilaslan K, Boyaci IH, Topcu A (2015) Rapid analysis of glucose, fructose and sucrose contents of commercial soft drinks using Raman spectroscopy. Food Control 48:56–61. doi:10.1016/j.foodcont.2014.01.001

Ma F, Liu D (2012) Sketch of the edible bird's nest and its important bioactivities. Food Res Int 48:559–567. doi:10.1016/j.foodres.2012.06.001

Marcone MF (2005) Characterization of the edible bird's nest the "Caviar of the East". Food Res Int 38:1125–1134. doi:10.1016/j.foodres.2005.02.008

Martin C, Bruneel J-L, Guyon F, Médina B, Jourdes M, Teissedre P-L, Guillaume F (2015) Raman spectroscopy of white wines. Food Chem 181:235–240. doi:10.1016/j.foodchem.2015.02.076

Mathlouthi M, Vinh Luu D (1980) Laser-raman spectra of D-glucose and sucrose in aqueous solution. Carbohydr Res 81:203–212. doi:10.1016/S0008-6215(00)85652-9

Nguyen TT, Gobinet C, Feru J, Pasco SB, Manfait M, Piot O (2012) Characterization of Type I and IV Collagens by Raman Microspectroscopy: identification of spectral markers of the dermo-epidermal junction. Spectrosc Int J 27:7. doi:10.1155/2012/686183

Pereira L, Sousa A, Coelho H, Amado AM, Ribeiro-Claro PJA (2003) Use of FTIR, FT-Raman and 13C-NMR spectroscopy for identification of some seaweed phycocolloids. Biomol Eng 20:223–228. doi:10.1016/S1389-0344(03)00058-3

Söderholm S, Roos YH, Meinander N, Hotokka M (1999) Raman spectra of fructose and glucose in the amorphous and crystalline states. J Raman Spectrosc 30:1009–1018

Vimala B, Hussain H, Nazaimoon WMW (2012) Effects of edible bird's nest on tumour necrosis factor-alpha secretion, nitric oxide production and cell viability of lipopolysaccharide-stimulated RAW 264.7 macrophages. Food Agric Immunol 23:303–314. doi:10.1080/09540105.2011.625494

Vinogradova E, Tlahuice-Flores A, Velazquez-Salazar JJ, Larios-Rodriguez E, Jose-Yacaman M (2014) Surface-enhanced Raman scattering of N-acetylneuraminic acid on silver nanoparticle surface. J Raman Spectrosc 45:730–735. doi:10.1002/jrs.4544

Wang CC (1921) The composition of Chinese edible bird's nest and the nature of their proteins. J Biol Chem 49:429–439

Wieruszeski JM et al (1987) Structure of the monosialyl oligosaccharides derived from salivary gland mucin glycoproteins of the Chinese swiftlet (genus Collocalia). Characterization of novel types of extended core structure, Gal beta(1—3)[GlcNAc beta(1—6)] GalNAc alpha(1—3)GalNAc(–ol), and of chain termination, [Gal alpha(1—4)]0–1[Gal beta(1—4)]2GlcNAc beta(1—.). J Biol Chem 262:6650–6657

Yang D, Ying Y (2011) Applications of Raman spectroscopy in agricultural products and food analysis: a review. Appl Spectrosc Rev 46:539–560. doi:10.1080/05704928.2011.593216

Yang M, Cheung S-H, Li SC, Cheung H-Y (2014) Establishment of a holistic and scientific protocol for the authentication and quality assurance of edible bird's nest. Food Chem 151:271–278. doi:10.1016/j.foodchem.2013.11.007

Zhang S et al (2013) Development of monoclonal antibodies and quantitative sandwich enxyme linked immunosorbent assay for the characteristic sialoglycoprotein of Edible bird's nest. J Immunoass Immunochem 34:49–60. doi:10.1080/15321819.2012.680527